



# Mesoscale Modeling of the Mouse Brain in different states of consciousness

By

Lakshika Rathi

Supervisor:

Prof. Saurabh Gandhi

Complex Systems and Neural Dynamics Lab

Bachelor Thesis

Sunday 29<sup>th</sup> September, 2024

---

## **Abstract**

This work is an attempt to model the mouse brain in different states of consciousness using a recently developed technique - Current Based Decomposition (CURBD). This would help to identify the differences in the inter-connections between the various brain regions in the awake versus the anaesthetized states. Consequently, this would give a deeper insight on the working mechanism of anaesthesia. We apply the CURBD technique to Gaussian-smoothed spiking data sampled at a rate of 200 Hz for mice under electrical and sensory stimulations. We further analyse the inter-connectivity matrices and observe the cortico-cortical and cortico-thalamic activities in both the awake and anaesthetized states.

---

## Acknowledgements

I would like to express an immense thank you to my thesis supervisor: Prof. Saurabh Gandhi. His support throughout the execution of this project has been invaluable. It has been an amazing experience working under him in parallel with another Masters student: Avinash Ranjan.

I am also grateful to the presentation committee: Prof. Lalan Kumar and Prof. Tapan Kumar Gandhi for their valuable feedback during the mid-term evaluations.

# Contents

<b>1</b>	<b>Introduction</b>	<b>1</b>
1.1	Consciousness . . . . .	1
1.2	Anesthesia and Human Brain . . . . .	1
1.3	Our Aim . . . . .	2
<b>2</b>	<b>Current Based Decomposition</b>	<b>3</b>
2.1	Introduction . . . . .	3
2.2	The use of RNNs . . . . .	3
2.3	The implementation . . . . .	4
<b>3</b>	<b>Dataset Description</b>	<b>6</b>
3.1	Introduction . . . . .	6
3.2	Data Collection Method . . . . .	6
3.3	Data Observations . . . . .	8
<b>4</b>	<b>Method Description</b>	<b>9</b>
4.1	Introduction . . . . .	9
4.2	Activity Data Pre-processing . . . . .	9
4.3	Current Based Decomposition . . . . .	10
4.4	Simulation to validate CURBD . . . . .	11
<b>5</b>	<b>Results</b>	<b>14</b>
5.1	Introduction . . . . .	14

<b>6 Interpretation</b>	<b>19</b>
6.1 Introduction . . . . .	19
6.2 Observations . . . . .	19
6.2.1 Mouse 599975 . . . . .	19
6.2.2 Mouse 586468 . . . . .	20
6.3 Definitive Regions of Difference . . . . .	21
<b>7 Future Directions</b>	<b>22</b>
7.1 Introduction . . . . .	22
7.2 Generalization of Difference regions . . . . .	22
7.3 Using the anatomically available connections . . . . .	22
7.4 Verification of CURBD through Simulation . . . . .	23
<b>8 Supplemental Figures</b>	<b>25</b>

# List of Figures

1.1	General Anesthesia and Human Brain Connectivity . . . . .	2
2.1	Current Based Decomposition, Courtesy-(2) . . . . .	4
2.2	Implementation of CURBD, Courtesy-(2) . . . . .	5
3.1	The multi-electrode array, Courtesy-(2) . . . . .	7
3.2	Spiking data from different probes, Courtesy-(2) . . . . .	8
4.1	Gaussian Smoothened Data . . . . .	10
4.2	Predicted Activity Data . . . . .	11
4.3	Interconnectivity Matrix Distribution . . . . .	12
4.4	Simulated Activity with Gaussian Distributed Interconnectivity Matrix	13
4.5	Simulated Activity with Exponentially Distributed Interconnectivity Matrix . . . . .	13
5.1	Mouse 599975, Awake and Anaesthetized state . . . . .	15
5.2	Mouse 599975, Difference between Awake and Anaesthetized state . . .	16
5.3	Mouse 586468, Awake and Anaesthetized states . . . . .	17
5.4	Mouse 586468, Difference between Awake states and Anaesthetized states	18
5.5	Mouse 586468, Difference between Awake and Anaesthetized state . . .	18
7.1	Anatomically Available Connections, Courtesy - (5) . . . . .	23
8.1	Mouse 599975, Awake and Anaesthetized State, Current=30uA . . . .	26

8.2	Mouse 599975, Difference between Awake and Anaesthetized State, Current=30uA . . . . .	27
8.3	Mouse 599975, Awake and Anaesthetized State, Current=70uA . . . . .	28
8.4	Mouse 599975, Difference between Awake and Anaesthetized State, Current=70uA . . . . .	29
8.5	Mouse 599975, Awake and Anaesthetized State, Sensory Stimulation . . . . .	30
8.6	Mouse 599975, Difference between Awake and Anaesthetized State, Sensory Stimulation . . . . .	31
8.7	Mouse 586468, Awake and Anaesthetized State, Current=25uA . . . . .	32
8.8	Mouse 586468, Difference between Awake states and Anaesthetized states, Current=25uA . . . . .	33
8.9	Mouse 586468, Difference between Awake and Anaesthetized state, Current=25uA . . . . .	33
8.10	Mouse 586468, Awake and Anaesthetized State, Current=45uA . . . . .	34
8.11	Mouse 586468, Difference between Awake states and Anaesthetized states, Current=45uA . . . . .	35
8.12	Mouse 586468, Difference between Awake and Anaesthetized state, Current=45uA . . . . .	35
8.13	Mouse 586468, Awake and Anaesthetized State, Sensory Stimulation . . . . .	36
8.14	Mouse 586468, Difference between Awake states, Sensory Stimulation . . . . .	36

# **Chapter 1**

## **Introduction**

### **1.1 Consciousness**

Like any other behavior, consciousness can also be defined as a behavior controlled by the brain, opening up a question on how it is linked with neural connections and brain dynamics. Such a study has been performed on a human brain on different patients in clinical settings (2). The first set had adults with severe consciousness disorders after a brain injury, brain infections, or drugs or alcohol intoxication, who were stable but bedridden and disabled. The second set of patients had normal brain functioning and were undergoing surgery for fixing injuries, removing a cancerous cell, or fixing different body parts and were under anesthesia. To prepare a consciousness test, their brains were zapped with Transcranial magnetic stimulation (TMS) in conscious and unconscious states, detecting the brain activity with an EEG which was analyzed with a data compression algorithm. The EEGs were assessed by a value called Perturbational Complexity Index (PCI), where the unconscious subjects were shown to have low scores.

### **1.2 Anesthesia and Human Brain**

As shown in (3), the effect of anesthesia on the human brain has been studied for decades in neuroscience. It has been shown that anesthesia substantially reduces cere-

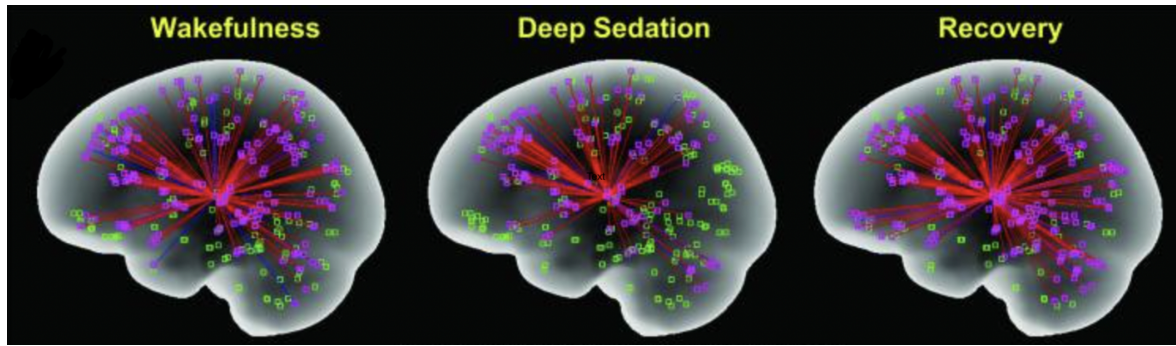


Figure 1.1: General Anesthesia and Human Brain Connectivity

bral metabolic rate and brain-wide connectivity. Figure 1.1 depicts the human brain in three different states - wakefulness, deep sedation, and recovery. The point of origin of the cluster of red lines is the thalamic nuclei while the red lines are thalamocortical connections. The pink squares represent the functionally connected areas of the neocortex while the green squares represent the functionally disconnected areas. This figure aptly captures the reduced thalamic-cortical functional connectivity under anesthesia. It also justifies one of the hypotheses of anesthesia under the unified theory of consciousness, “reduced thalamocortical functional connectivity” under anesthesia.

### 1.3 Our Aim

We aim to replicate such experiments on mice brain. We characterize the flow of information between neurons in different states of consciousness from awake to anesthetized with the help of functional connectivity matrices. This study will give an in-depth view on the mechanisms of anesthesia and also improve our general ability to monitor anesthesia.

# Chapter 2

## Current Based Decomposition

### 2.1 Introduction

During various activities, the different regions of the brain interact with each other establishing macroscopic circuits which are connected recurrently directly through direct projections and multi-synapse loops, and indirectly by neuromodulator release. The paper by Matthew G. Perich, et al (1), introduces a novel technique called CURBD or Current-Based decomposition for inferring brain-wide interactions. CURBD is a computational framework that uses recurrent neural networks or RNNs and reproduces the experimentally-obtained neural data.

### 2.2 The use of RNNs

The development of CURBD was based on the idea that the current exchange between the active units in an RNN can be found out precisely. Say, we study a single target unit being driven by multiple source units as in 2.1a, then it can be modeled as the sum of effect of all the source neurons being weighted by their activity. Scaling this to multiple units as in 2.1b, we can extend the same concept and compute the activity of any particular unit as the sum of all the other units connected to it weighted by their activity. Mathematically, this can be represented as a matrix of dimension MxN where

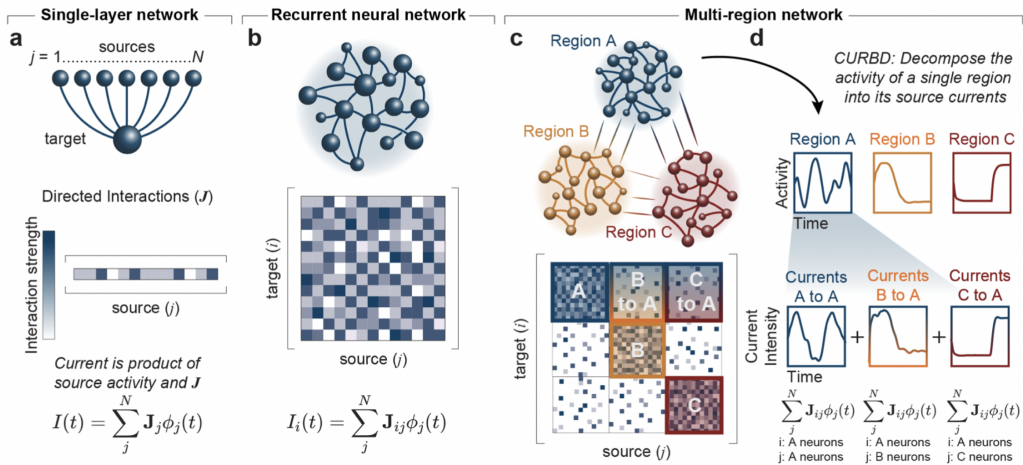


Figure 2.1: Current Based Decomposition, Courtesy-(2)

$N$  is the number of source units and  $M$  is the number of target units. The numerical value represents the strength of the connection and the direction (positive or negative) represents excitatory or inhibitory neural connections.

Different regions of the brain are interconnected with each other, this technique represents each region of the brain as a single RNN. The entire brain is thus represented as multiple RNNs interconnected to each other, forming a “network of networks” model. Each unit in a region is driven by inputs from all regions connected to it as well as the connected units connected to it recurrently within the same region. In any target region, the source currents are given by the submatrix from the complete directed interaction matrix as shown in 2.1c. The different submatrices thus help to decompose the total activity of any region into the source currents driving it from all other regions as in 2.1d.

## 2.3 The implementation

CURBD is effectively based upon the directed interaction matrix  $J$ , which depicts the strength as well as type - excitatory ( $J_{ij} > 0$ ) or inhibitory ( $J_{ij} < 0$ ) - of interactions between neurons. This is inferred from multi-region experimental data modeled as RNNs as described in the section above. Without taking into account the different

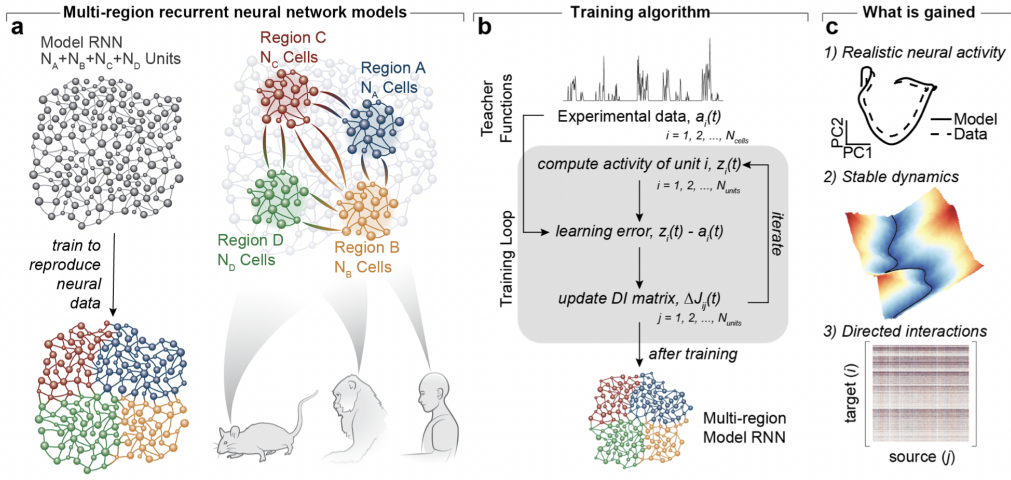


Figure 2.2: Implementation of CURBD, Courtesy-(2)

regions, the model RNN is initialized with an initial number of units equal to the total number of neurons in the dataset. The end goal is to learn the directed interaction matrix given only the initial state of activity of the neurons. The activity of the next time step is given as the sum of the current state of activity of the source neurons,  $\phi(t)$  weighted by J.

$$\phi_i(t) = \sum_j^N J_{ij} \phi_j(t) \quad (2.1)$$

The training is done iteratively as in 2.2b, minimizing the linear error between a model RNN unit ( $z_i(t)$ ) and the experimentally recorded activity of that unit ( $a_i(t)$ ). At each time step, the matrix J is updated as

$$J(t+1) = J(t) + \Delta J(t) \quad (2.2)$$

The Model RNN doesn't need to differentiate between different regions and is learned as a single dynamical system. The model RNN generates realistic patterns of the neural activity shows stable dynamics and estimates the directed interactions between different neurons. The directed interactions are an estimate of the functional interactions between different neurons.

# Chapter 3

## Dataset Description

### 3.1 Introduction

One of the first contenders to discover biomarkers of the state of consciousness is Electroencephalography or EEG. However, spontaneous EEG can show high false alarms while diagnosing patients with consciousness disorders leading to very unusual spatio-temporal patterns. The more promising candidate in this regard is perturbational EEG where the cortical activity in the brain is recorded by probing it with a brief magnetical pulse. This is followed by measuring the spatio-temporal complexity known as perturbational complexity analysis. The dataset used in the project is collected using a similar method by scientists of the Mindscope Program, Allen Institute, Seattle (3).

### 3.2 Data Collection Method

The underlying neural connections in mice were examined using EEG along with Neuropixels probes in awake mice and in mice anesthetized with isoflurane. The Neuropixels probes have the capacity to record and access the intra-areal and inter-areal dynamics underlying the EEG signals, helping us investigate the cortico-cortical and cortico-thalamic activity.

Figure 3.1 shows a schematic of the multi-electrode array with 30 channels implanted

on the skull top over the major areas - motor, somatosensory, visual, and retrosplenial areas.

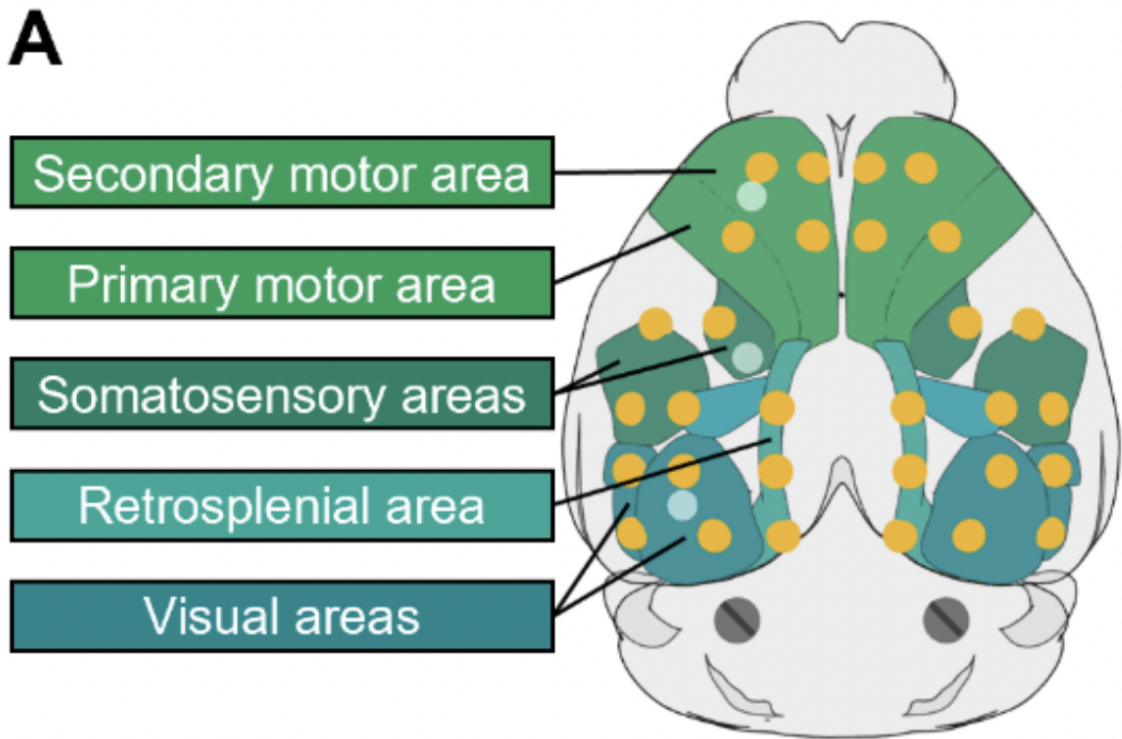


Figure 3.1: The multi-electrode array, Courtesy-([2](#))

Both the spiking response pattern and EEG signals were recorded. It has data from up to three Neuropixels probes which capture the local field potential (LFP) and action potentials. To observe the LFP and spiking activity in individual neurons, the neuropixels probes were placed in a manner to record data from the cortical region (Motor MO, Anterior Cingulate ACA, Somatosensory SS and Visual VIS) and the sesnsorimotor-related thalamic nuclei (SM-TH).

Figure [3.2](#) shows an example of data collected from a mouse brain using three Neuropixel probes - B, D, and F along with the labels marked for different regions.

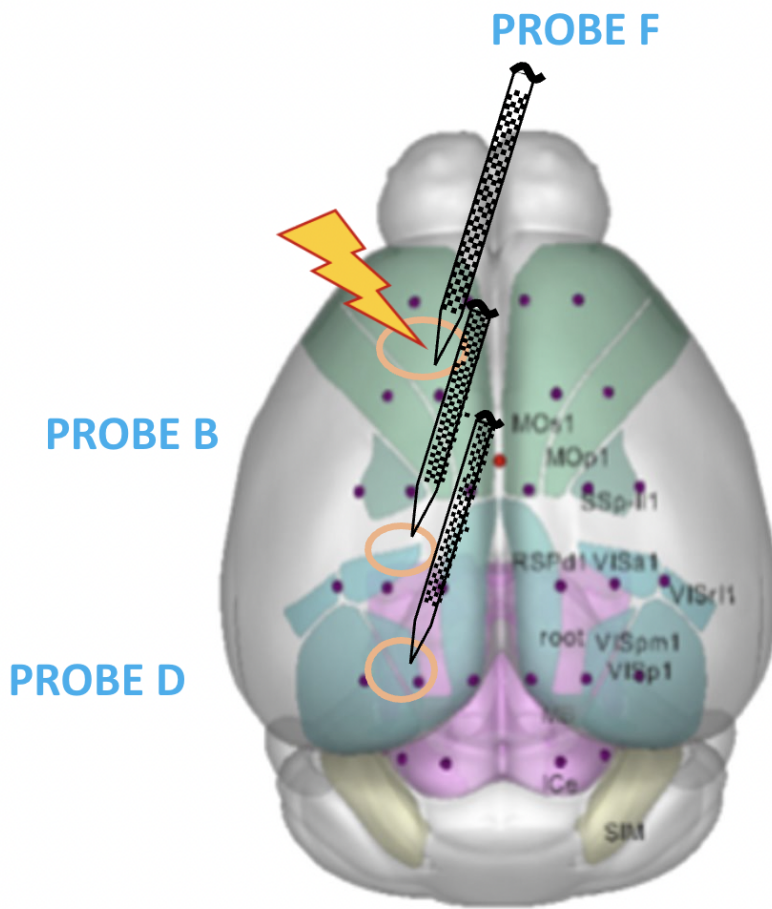


Figure 3.2: Spiking data from different probes, Courtesy-([2](#))

### 3.3 Data Observations

The stimulation of deep cortical layers in the awake state evokes a pulse of excitation, followed by a bi-phasic simulation of time period 120 milli-seconds and a rebound excitation phase. The same pattern seen in the thalamic nuclei is partially attributed to burst spiking. The cortical and thalamic off-period and the rebound excitation were absent in the anesthetized state.

# Chapter 4

## Method Description

### 4.1 Introduction

We use the spiking data from the mouse brain in different states of consciousness which act as the initial activity of the different neurons. This activity is then used to create a Multi-RNN network as used in CURBD, giving us a directed interaction matrix between the source and target neurons in different regions of the mouse brain.

### 4.2 Activity Data Pre-processing

As described above, the mouse brain is probed by a brief magnetical pulse of 0.0004 seconds, and the subsequent activity is recorded. For each stimulus, the data is recorded for 120 trials using two different kinds of stimulus - electrical and sensory. The electrical stimulation is again done at different values of currents.

We form an “average activity data” by using all 120 trials for different stimulations in intervals of 3.4 seconds right after the stimulation ends. The spiking data consists of discrete spikes recorded at different time points. To convert these discrete spikes into a continuous signal for CURBD, we perform binning by taking bins of size 5 milli-seconds in the 3.4 seconds interval and counting the number of spikes of a neuron in each bin. This gives us a continuous “firing rate” time series with a sampling rate of 200 Hz.

This binning is performed for all 120 trials in any stimulation and then averaged. To further remove the specific spike details and unnecessary noise, we gaussian-smoothen this activity data by convolving it with a gaussian fixed half-width of 25 milliseconds. This gives us continuous time-series data for 3.4 seconds, divided across 680 bins each of 5 milliseconds. Figure 4.1 shows an example of the activity data we use, where the blue data represents the average spiking data across the 120 trials and the orange data is the gaussian-smoothened version for a particular neuron.

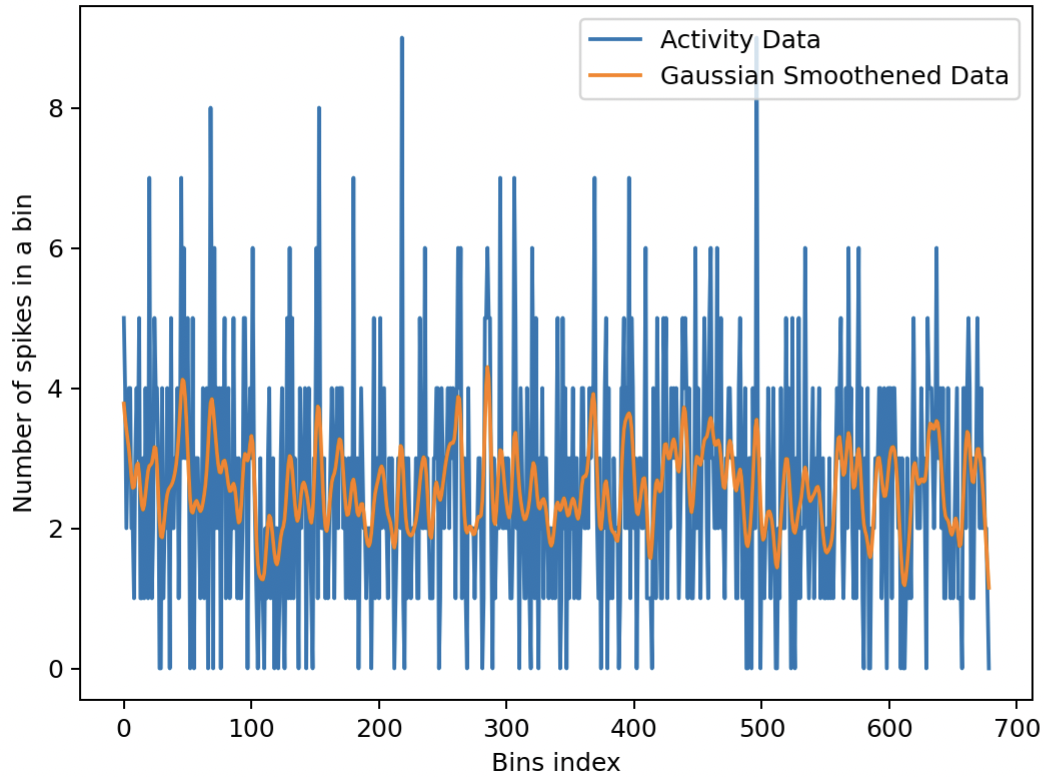


Figure 4.1: Gaussian Smoothened Data

### 4.3 Current Based Decomposition

The Gaussian-smoothened data is then fed as the initial activity for different source neurons in the CURBD Multi-RNN model. We use a strength of 1.5 for the recurrent

connections and an RNN unit-decay constant of 0.0075. The model was then trained for an average of 1000 epochs with a learning rate of 1.0, using the “tanh” non-linearity. This gave us a directed connection matrix of the source neurons with the target neurons. We analyzed the obtained matrix based on the connections between neurons in different regions in the awake and anesthetized states of consciousness.

## 4.4 Simulation to validate CURBD

To validate CURBD, the paper (1) creates a hypothetical dataset with 100 neurons and verifies if the method efficiently disentangles the inter-region connectivity. Along similar lines, we verify our simulated matrices as the initial connectivity matrix along with the initial activity data as the gaussian-smoothened data after doing its z-scoring and applying tanh non-linearity to restrict its range between -1 and 1. Unfortunately, the simulation-based method didn’t work well for us as the predicted activity data using this simulation goes flat after a brief bump in the beginning as in Figure 4.2.

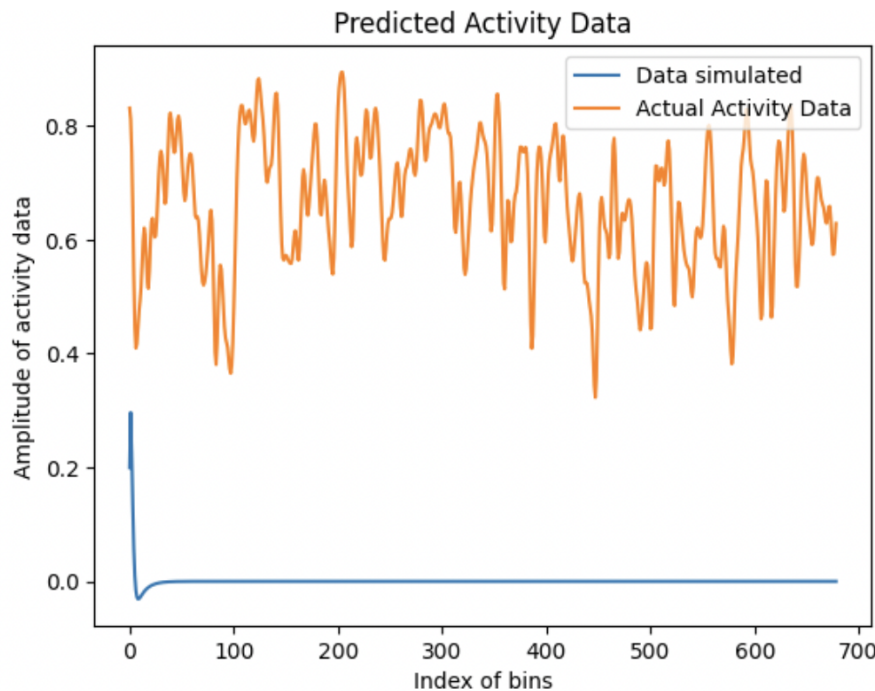


Figure 4.2: Predicted Activity Data

To dig deeper into this issue, we see the distribution of the interconnectivity matrix generated from our data and that used in the simulation method of the paper (1). We observe in Figure 4.3 that the simulation matrix used in the paper broadly shows a Gaussian distribution with a mean of zero while the matrix generated from our data has an exponential distribution with a mean of zero.

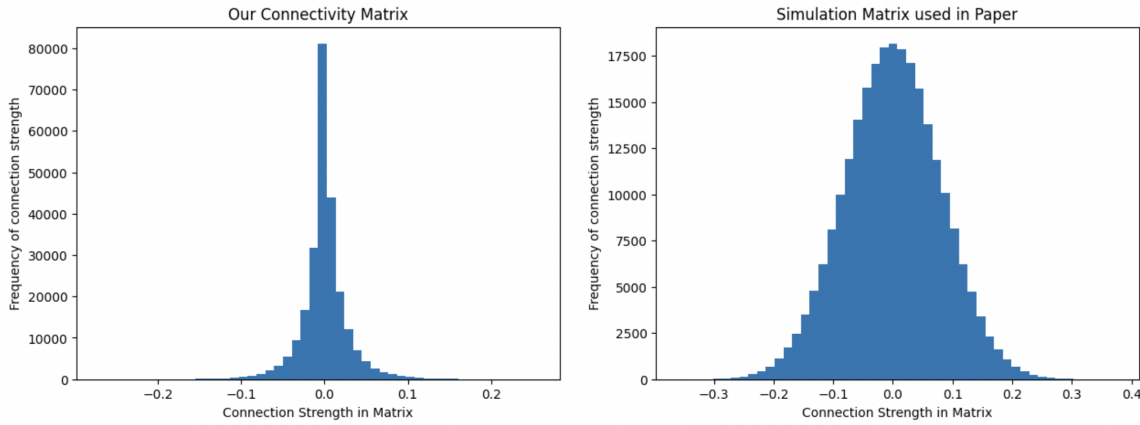


Figure 4.3: Interconnectivity Matrix Distribution

We also tried using their connectivity matrix (with a gaussian distribution) and the initial activity data as our gaussian-smoothed data and observe that the simulated activity data is no more a flat curve as in Figure 4.4

Next, we initialize the simulation model with our gaussian smoothed data but with an exponentially distributed connectivity matrix and again observe a flat curve as in Figure 4.5. We tried this experiment multiple times with different exponential constants but didn't succeed in any attempt.

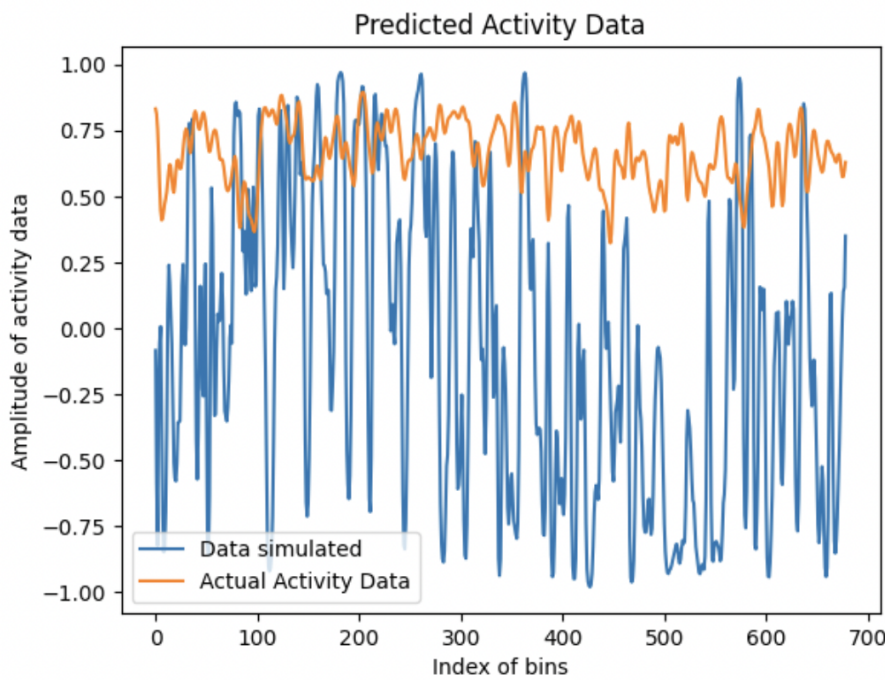


Figure 4.4: Simulated Activity with Gaussian Distributed Interconnectivity Matrix

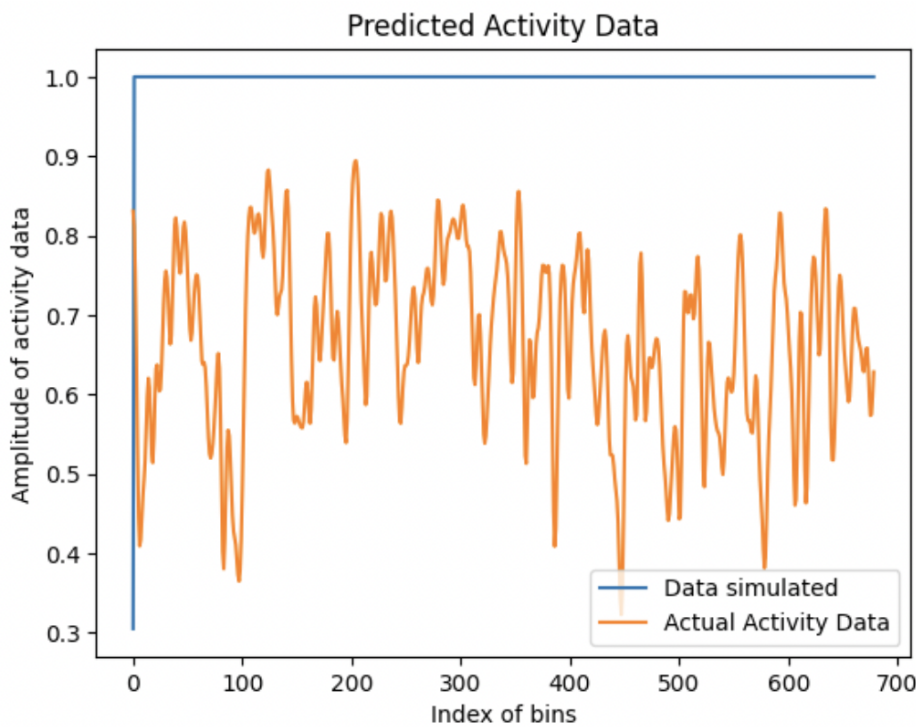


Figure 4.5: Simulated Activity with Exponentially Distributed Interconnectivity Matrix

# Chapter 5

## Results

### 5.1 Introduction

We performed the Current Based Decomposition for two mice from the dataset across different states of consciousness and different stimulations.

- Mouse 599975 - Awake and Anaesthetized State
  - Electrical Stimulation, current = 30 uA
  - Electrical Stimulation, current = 50 uA
  - Electrical Stimulation, current = 70 uA
  - Sensory Stimulation
- Mouse 586468 - Awake and Anaesthetized States
  - Electrical Stimulation, current = 25 uA
  - Electrical Stimulation, current = 35 uA
  - Electrical Stimulation, current = 45 uA
  - Sensory Stimulation

After training the multi-RNN network, the inter-connectivity matrices for the first mouse 599975 is shown in Figure 8.10.

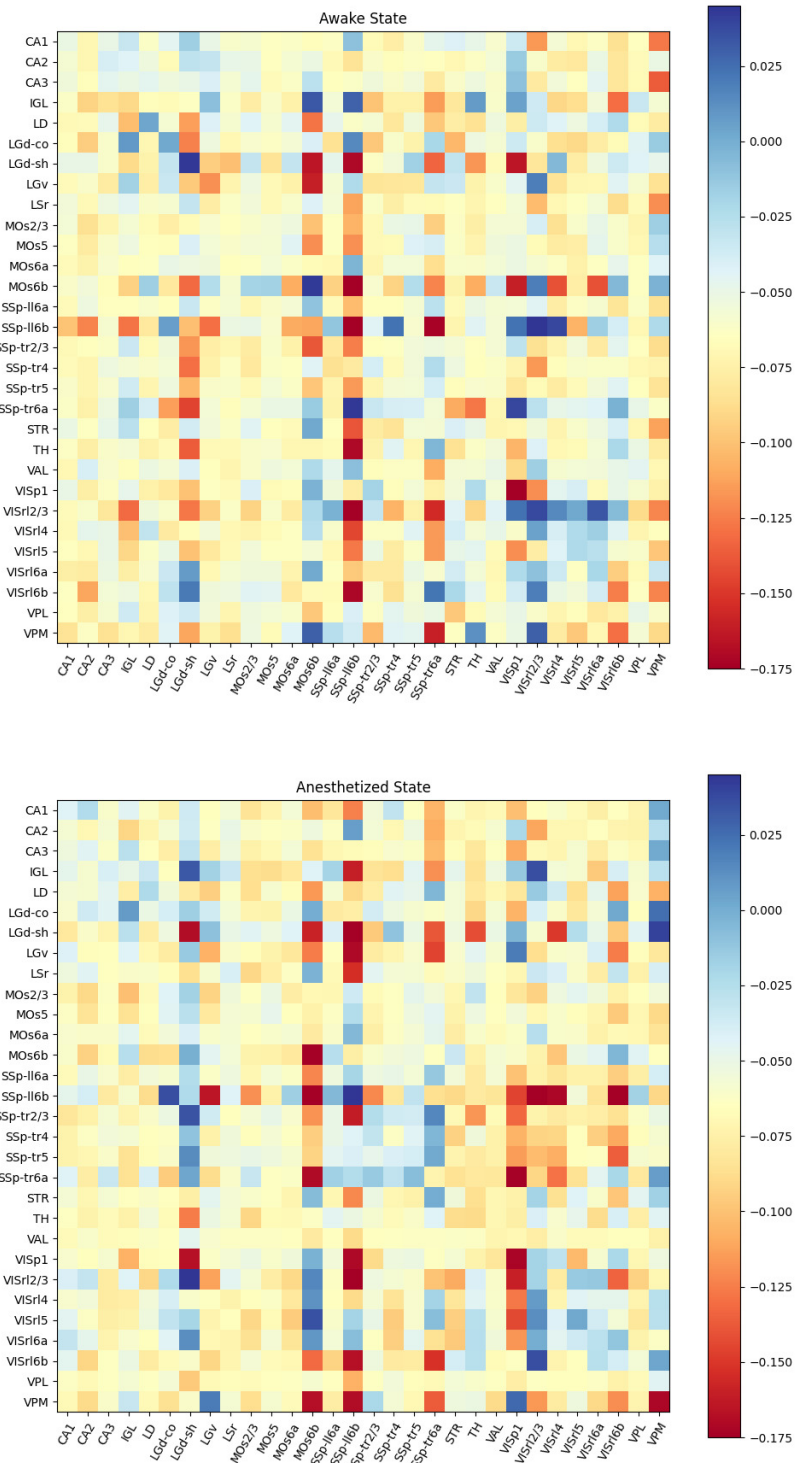


Figure 5.1: Mouse 599975, Awake and Anaesthetized state

To obtain a comparative analysis between the awake and the anaesthetized state, we plot the difference between the two inter-connectivity matrices in Figure 8.6.

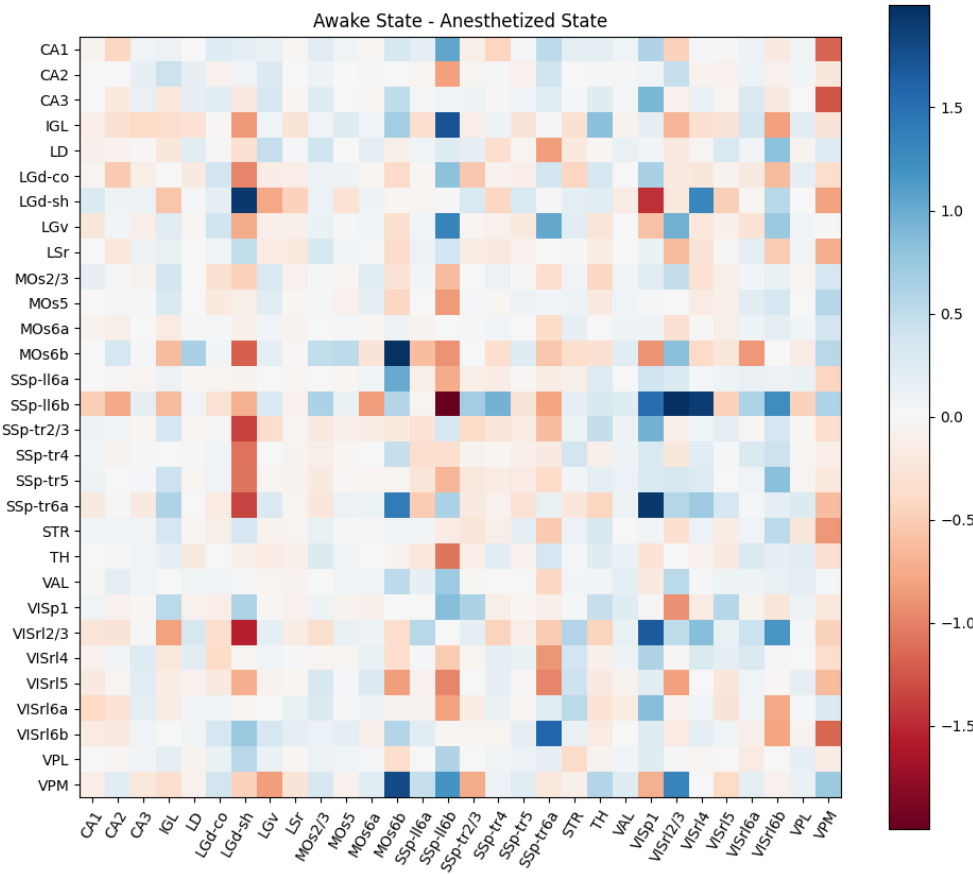


Figure 5.2: Mouse 599975, Difference between Awake and Anaesthetized state

The second mouse 586468 has four different kind of stimulations, the inter-connectivity matrices of which are shown in Figure 5.3.

To again compare between the different states, we plot the difference matrices between the two awake states, the two anaesthetized states in Figure 8.13 and an awake and anaesthetized state pair in Figure 8.14.

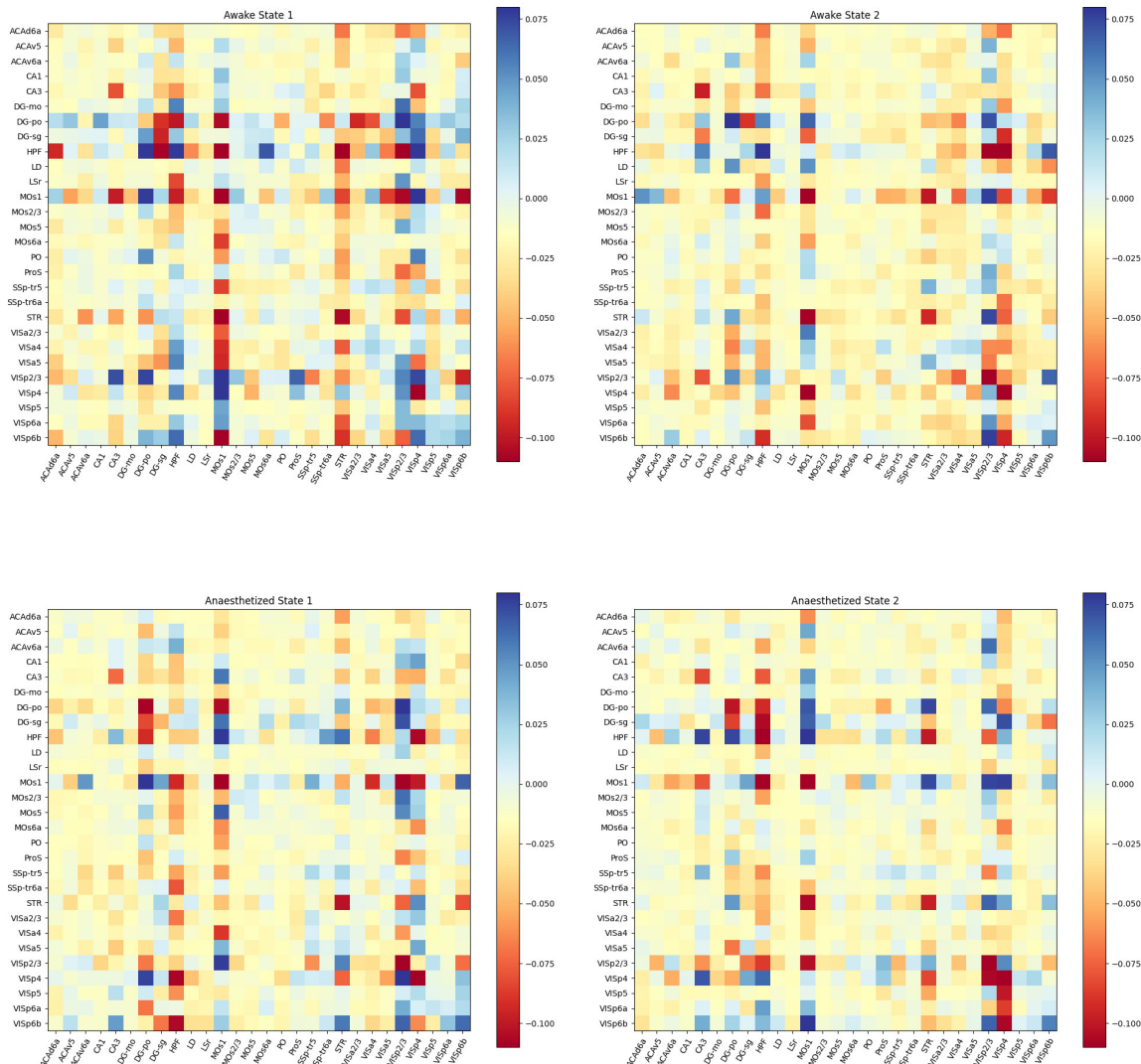


Figure 5.3: Mouse 586468, Awake and Anaesthetized states

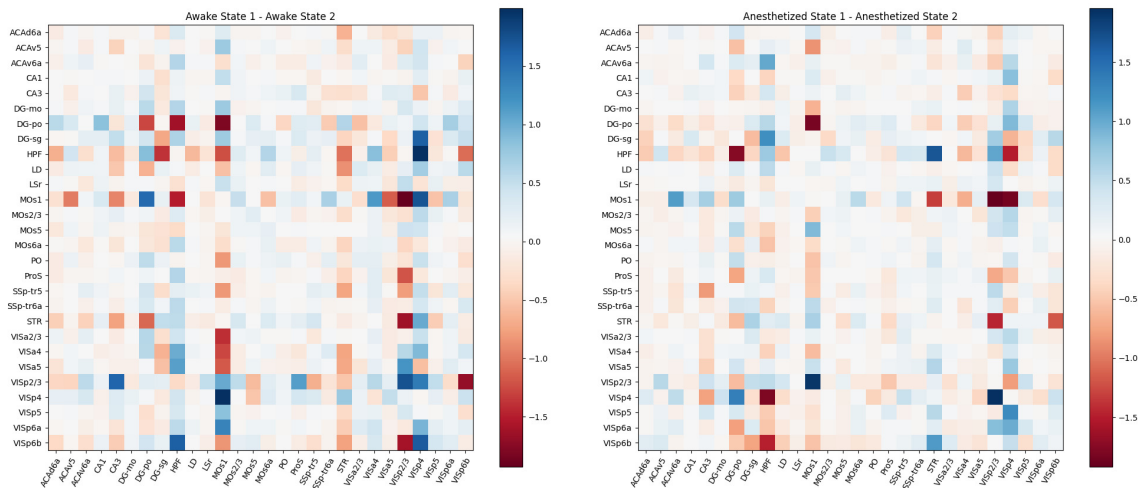


Figure 5.4: Mouse 586468, Difference between Awake states and Anaesthetized states

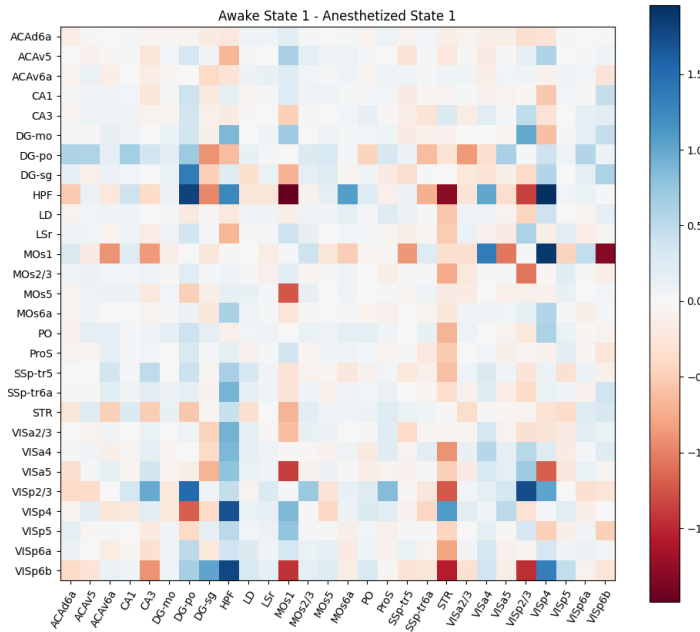


Figure 5.5: Mouse 586468, Difference between Awake and Anaesthetized state

# Chapter 6

## Interpretation

### 6.1 Introduction

To interpret the connectivity strength of the different regions of the mouse brain, we carefully analyse the inter-connectivity matrices obtained after training the multi-region RNN networks.

### 6.2 Observations

#### 6.2.1 Mouse 599975

Based on the Figure 8.10, we can make the following observations-

- The hippocampus regions (CA1, CA2, CA3) do not have very strong connections in either the awake or the anaesthetized state.
- The thalamic regions have weak connections except the region LGD-sh which shows very strong inhibitory connections in the awake state and much weaker excitatory connections in the anaesthetized state.
- In the motor areas of the cortex, the region MOs6b shows strong connections in both the awake and anaesthetized states.

- Similarly, in the somatosensory areas of the cortex, the SSp-ll6b and SSp-tr6a show significant connections in both states of consciousness.
- The visual areas of cortex shows strong connections in the VISp1 and VISp2/3 regions.

These observations are also verified by the difference matrix in Figure 8.6.

### 6.2.2 Mouse 586468

Similarly, we study the Figure 5.3, to make observations based on the inter-connectivity matrices of the 2nd mouse in the four states of consciousness shown.

- The hippocampus regions (CA1, CA3, LD, LSr) have weak connections in all the states except for some strong connections in the CA3 region in the awake states.
- The dentate gyrus regions uniformly show strong connections for the DG-po region and a few strong connections for DG-sg in the awake state-1.
- The hippocampal formation region (HPF) is seen to have significant connections with the other regions in all the four states.
- The motor regions of the cortex show strong connections only for the MOs1 region in all the four states shown.
- The striatum (region) shows significantly strong connections in the awake state 1 and a few connections in the two anaesthetized states shown.
- The visual regions of the cortex show significant connections in the VISp2/3 and VISp4 regions in all the four states and a few weak connections in the VISp6b region.

The difference matrices between the awake states and between the anaesthetized states as in Figure 8.13, reflect these differences. The difference between an awake and an anaesthetized states in Figure 8.14, represents the stark differences in different regions of the mouse brain.

## 6.3 Definitive Regions of Difference

From the individual analysis of the inter-connectivity matrices of the two mice in the section above, we can make some concluding interpretations -

- The hippocampus regions of the brain show weak connections in both the awake and the anaesthetized state.
- The cortical connections of significant magnitude are majorly present in the -
  - Motor Region (MOs1, MOs6b)
  - Visual Regions (ViSp1, ViSp2/3, ViSp4)
- Some regions show significant difference in their connection strengths between the awake and the anaesthetized states.

# **Chapter 7**

## **Future Directions**

### **7.1 Introduction**

This work gives a brief insight on the potential of the Current Based Decomposition Method to predict the inter-connectivity strength between different brain regions.

### **7.2 Generalization of Difference regions**

The work can be extended by applying the CURBD technique to multiple other mice, based on the dataset available from the Allen Institute. Analysing more inter-connectivity matrices would give a much stronger idea on the significant regions of differences between the different awake and anaesthetized states.

### **7.3 Using the anatomically available connections**

The paper (5), provides us information on the actual anatomical connections as seen in the mouse brain. To get a more accurate idea on the inter-connections, we can constrain our connection matrix to the anatomically available connections 7.1.

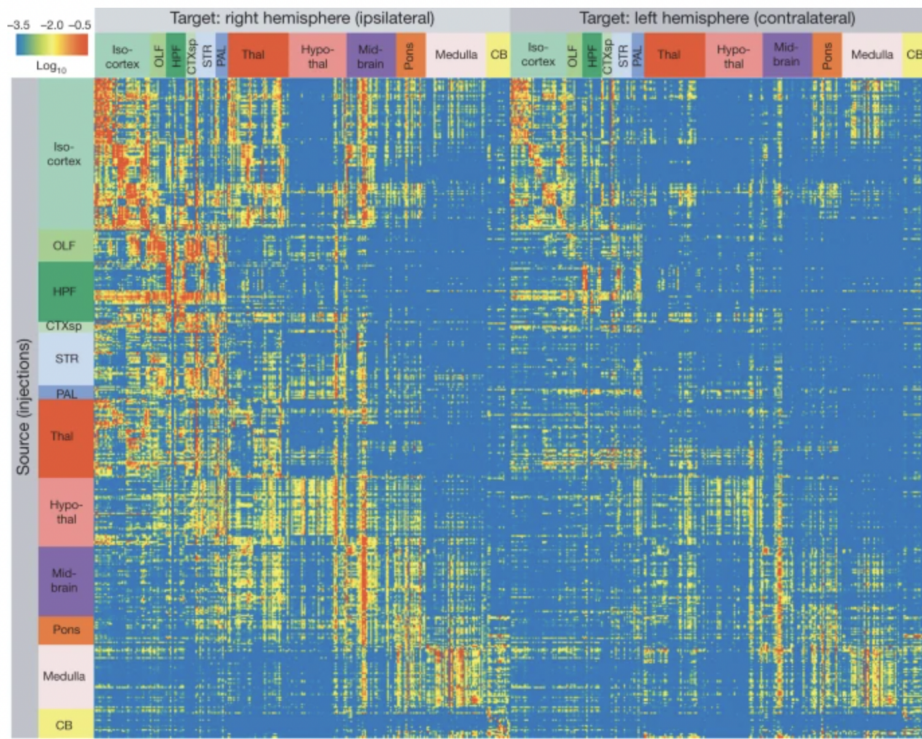


Figure 7.1: Anatomically Available Connections, Courtesy - (5)

## 7.4 Verification of CURBD through Simulation

As described in the Methods section, the CURBD technique can be validated by simulating the activity back from the given inter-connectivity matrix. The verification would be a boost to the observations we made, and is an important future direction.

# Bibliography

- [1] Matthew G. Perich, Charlotte Arlt, Sofia Soares, Megan E. Young, Clayton P. Mosher, Juri Minxha, Eugene Carter, Ueli Rutishauser, Peter H. Rudebeck, Christopher D. Harvey, Kanaka Rajan, [Inferring brain-wide interactions using data-constrained recurrent neural network models](#), 2021
- [2] Christof Koch, [How to make a Consciousness Meter](#), 2017
- [3] Anthony G. Hudetz, [General Anesthesia and Human Brain Connectivity](#), 2012
- [4] Leslie D. Claar, Irene Rembado, Jacqulyn R. Kuyat, Lydia C. Marks, Shawn R. Olsen, Christof Koch, [Cortico-thalamo-cortical interactions modulate electrically evoked EEG responses in mice](#), 2022
- [5] Seung Wook Oh, Julie A. Harris, Lydia Ng, Brent Winslow, Nicholas Cain, Stefan Mihalas, Quanxin Wang, Chris Lau, Leonard Kuan, Alex M. Henry, Marty T. Mortrud, Benjamin Ouellette, Thuc Nghi Nguyen, Staci A. Sorensen, Clifford R. Slaughterbeck, Wayne Wakeman, Yang Li, David Feng, Anh Ho, Eric Nicholas, Karla E. Hirokawa, Phillip Bohn, Kevin M. Joines, Hanchuan Peng, Michael J. Hawrylycz, John W. Phillips, John G. Hohmann, Paul Wohnoutka, Charles R. Gerfen, Christof Koch, Amy Bernard, Chinh Dang, Allan R. Jones Hongkui Zeng, [A mesoscale connectome of the mouse brain](#), 2014

# Chapter 8

## Supplemental Figures

We had trained the two mice for different types of simulations and this chapter includes all the inter-connectivity matrices obtained.

- Mouse 599975 - Awake and Anaesthetized State
  - Electrical Stimulation, current = 30 uA
  - Electrical Stimulation, current = 70 uA
  - Sensory Stimulation
- Mouse 586468 - Awake and Anaesthetized States
  - Electrical Stimulation, current = 25 uA
  - Electrical Stimulation, current = 45 uA
  - Sensory Stimulation

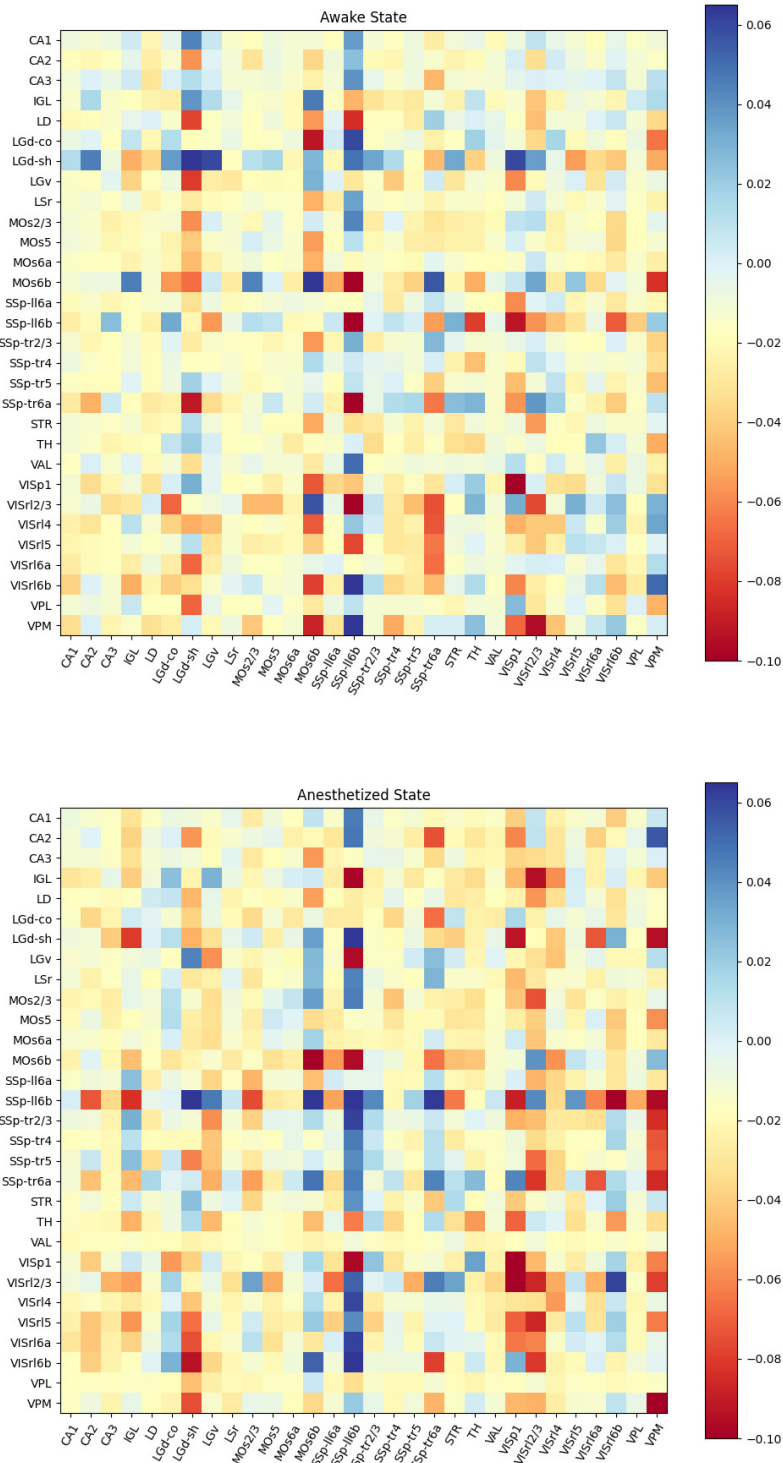


Figure 8.1: Mouse 599975, Awake and Anaesthetized State, Current=30uA

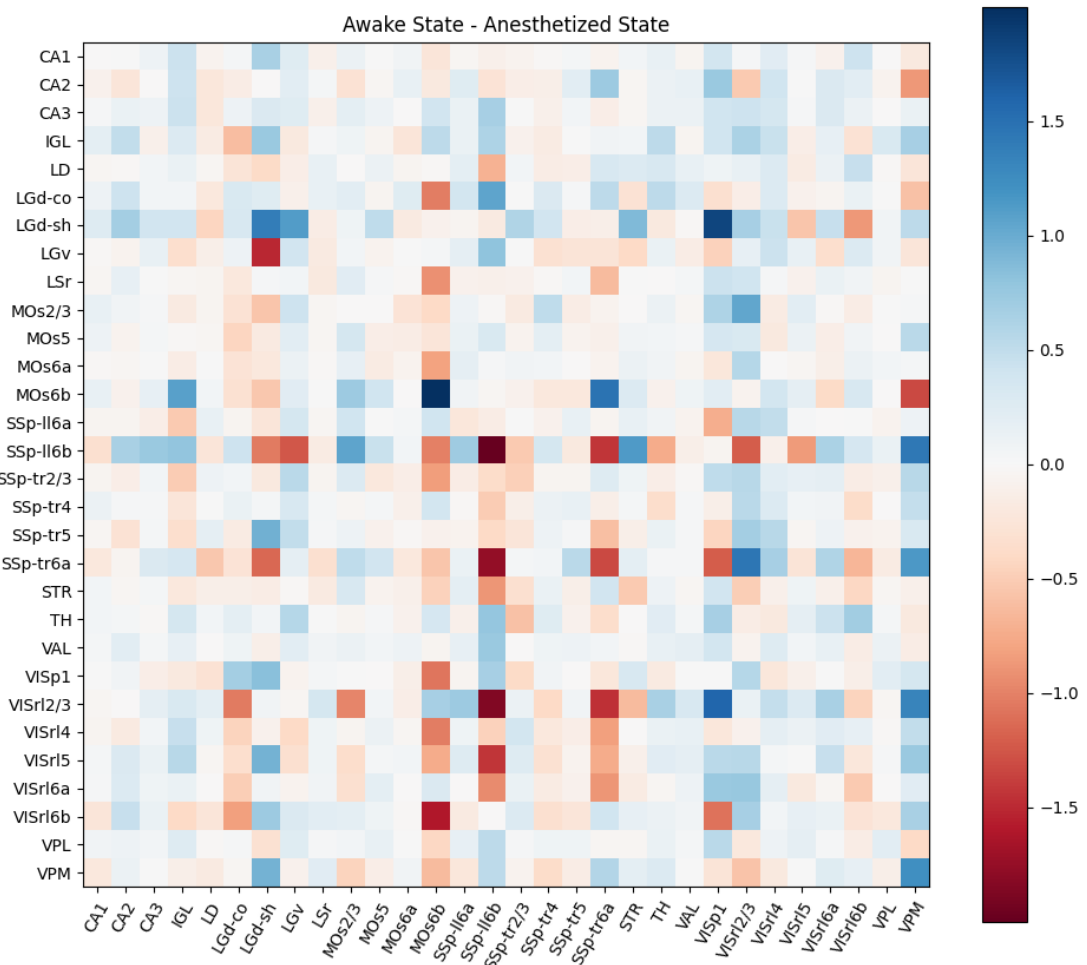


Figure 8.2: Mouse 599975, Difference between Awake and Anaesthetized State, Current=30uA

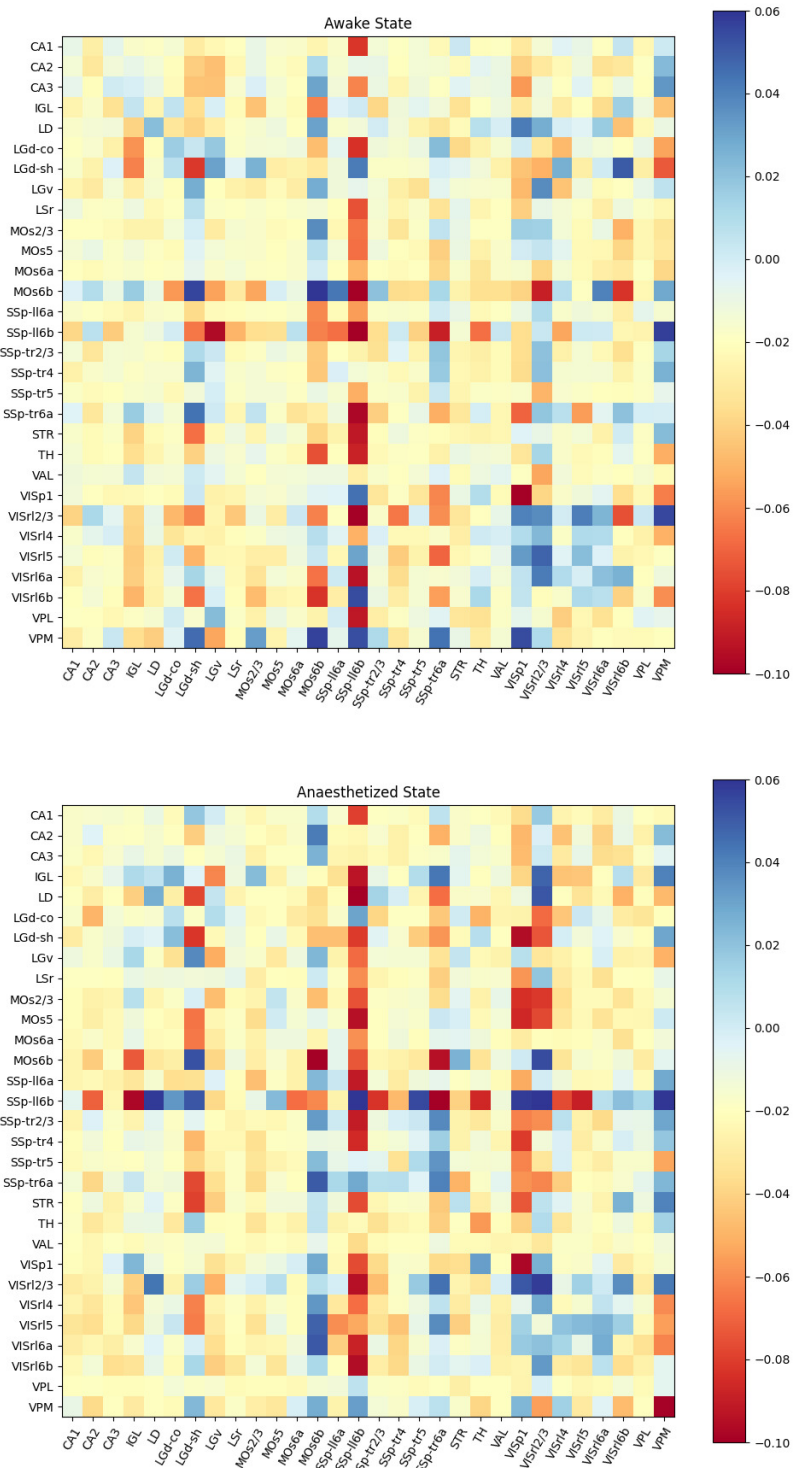


Figure 8.3: Mouse 599975, Awake and Anaesthetized State, Current=70uA

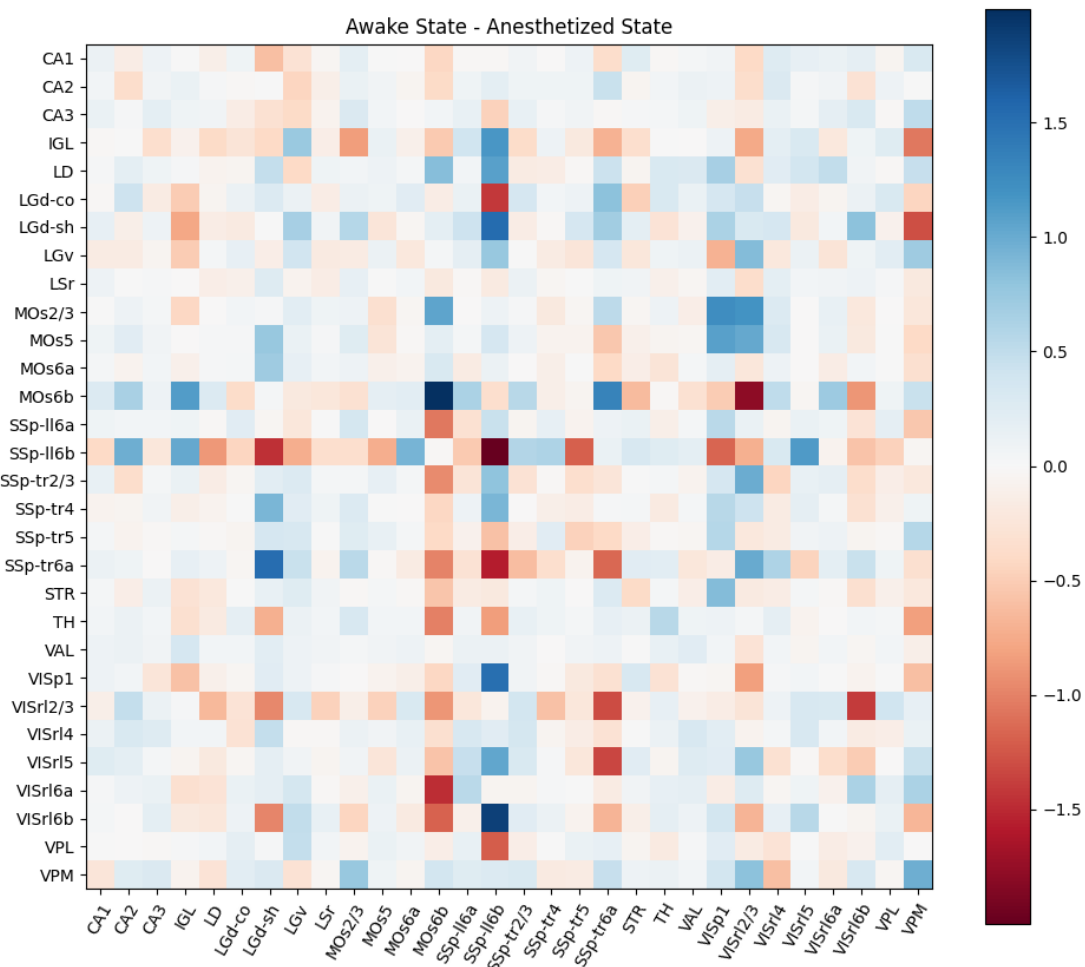


Figure 8.4: Mouse 599975, Difference between Awake and Anaesthetized State, Current=70uA

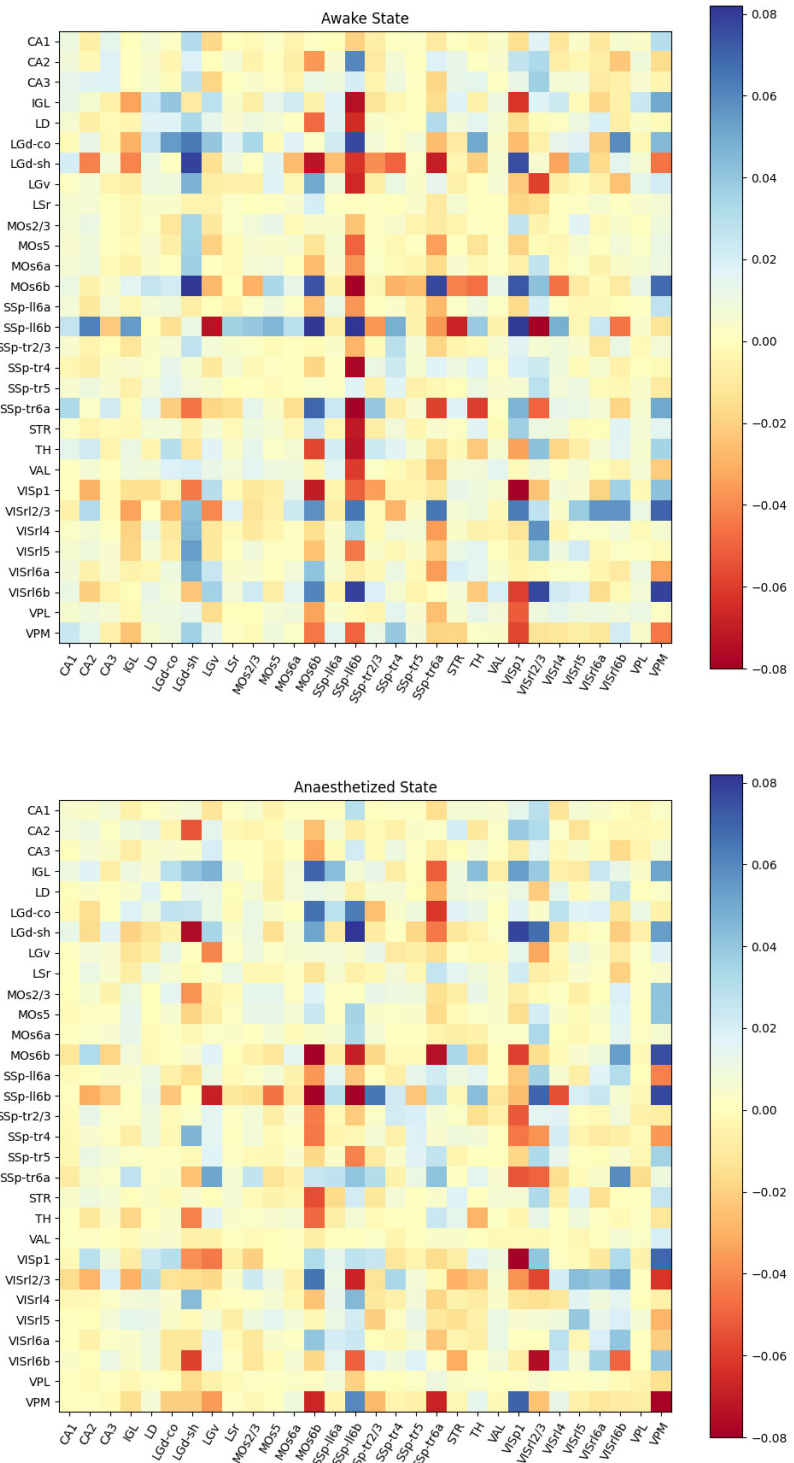


Figure 8.5: Mouse 599975, Awake and Anaesthetized State, Sensory Stimulation

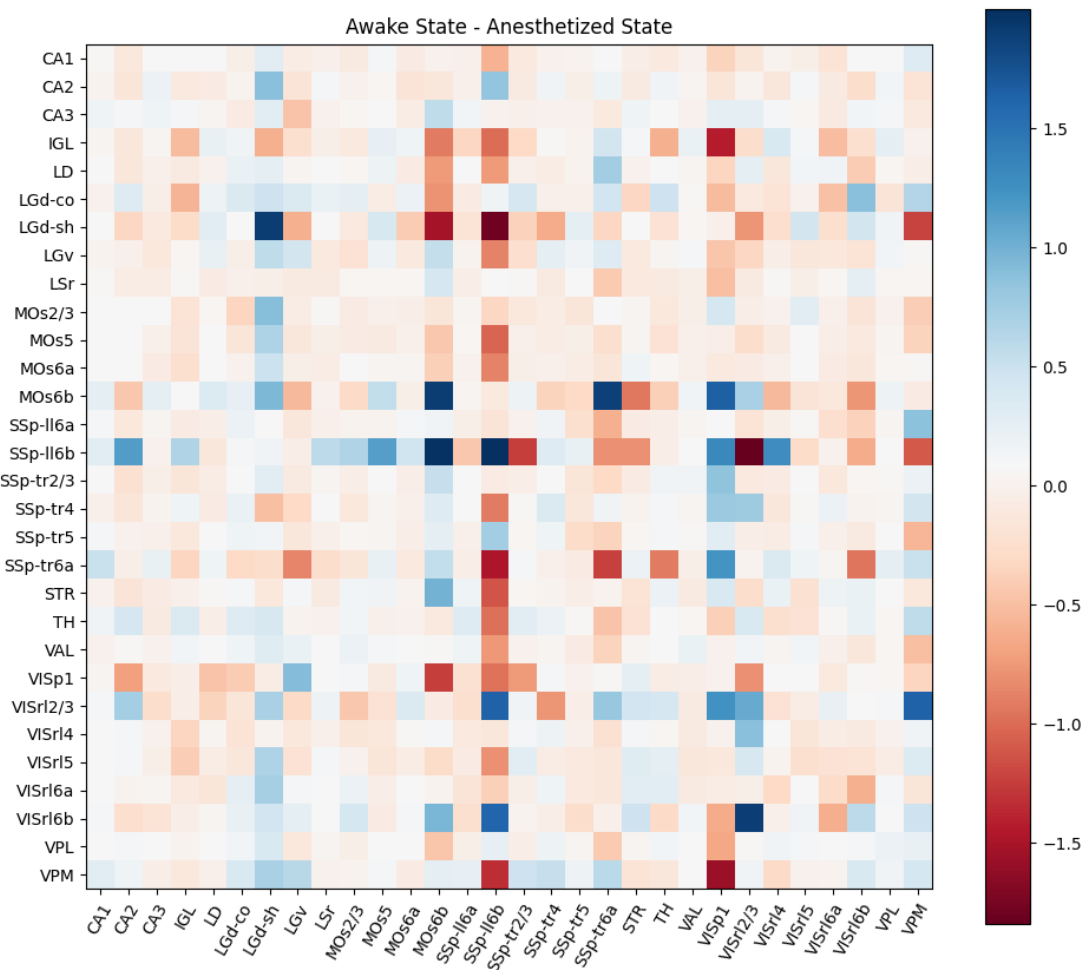


Figure 8.6: Mouse 599975, Difference between Awake and Anaesthetized State, Sensory Stimulation

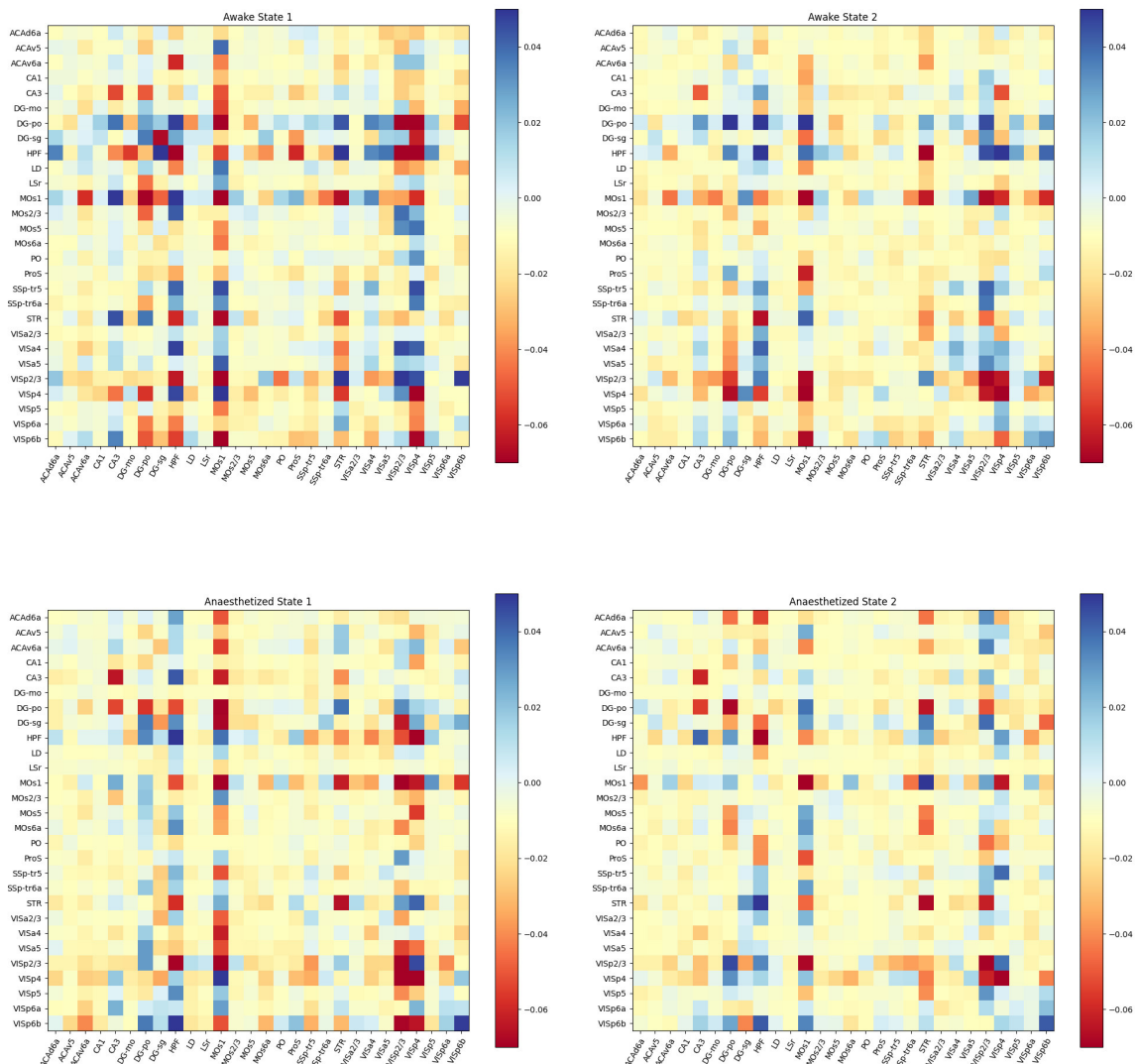


Figure 8.7: Mouse 586468, Awake and Anaesthetized State, Current=25uA

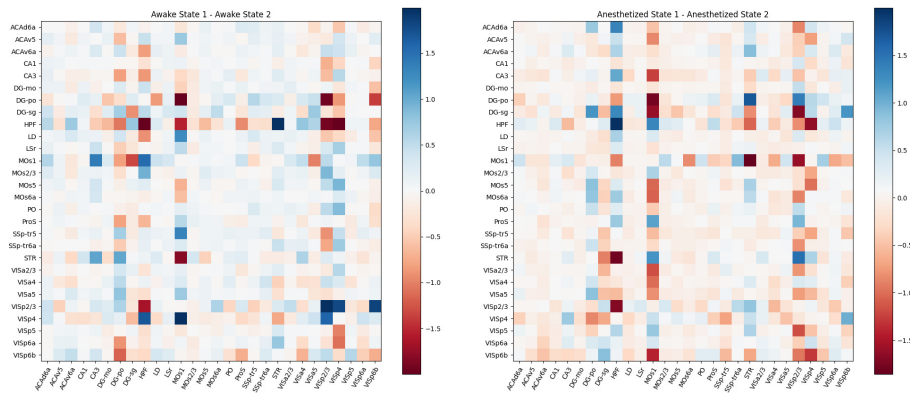


Figure 8.8: Mouse 586468, Difference between Awake states and Anaesthetized states, Current=25uA

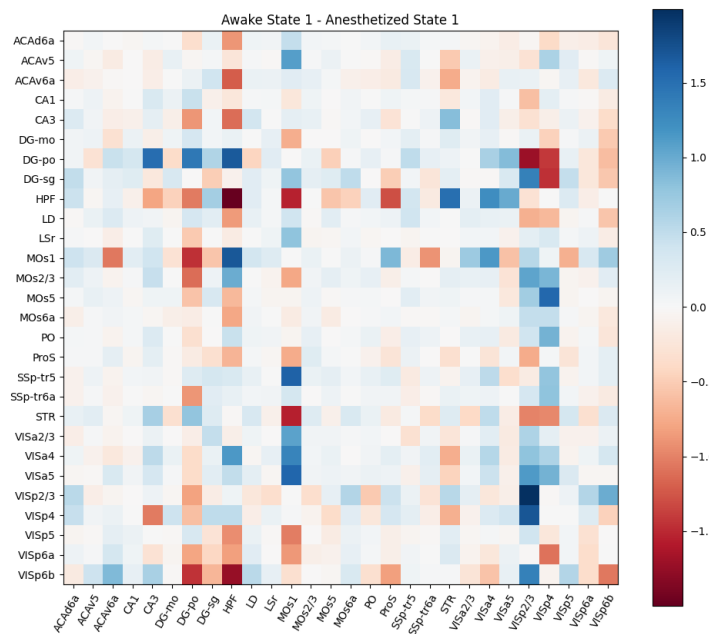


Figure 8.9: Mouse 586468, Difference between Awake and Anaesthetized state, Current=25uA

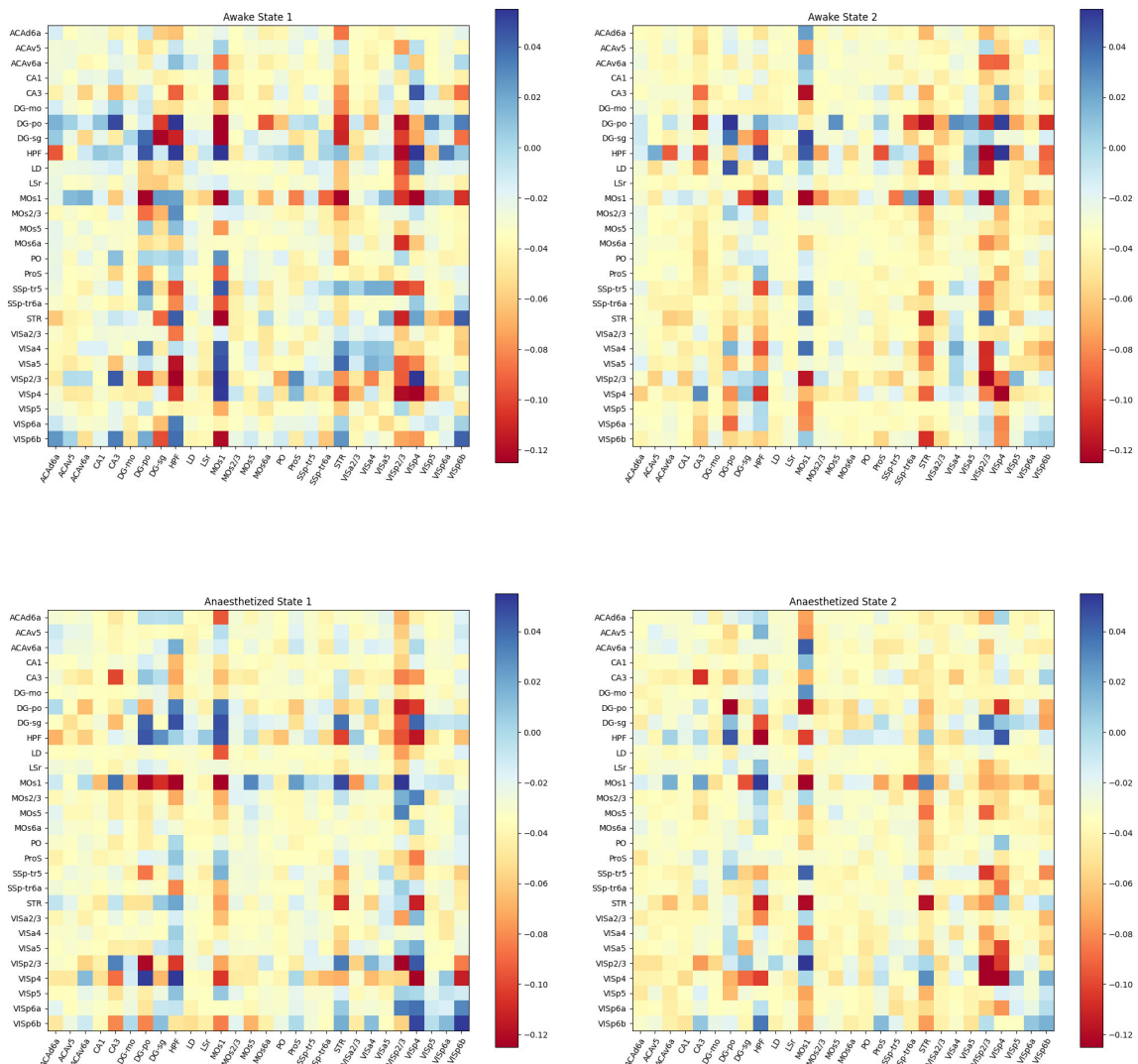


Figure 8.10: Mouse 586468, Awake and Anaesthetized State, Current=45uA

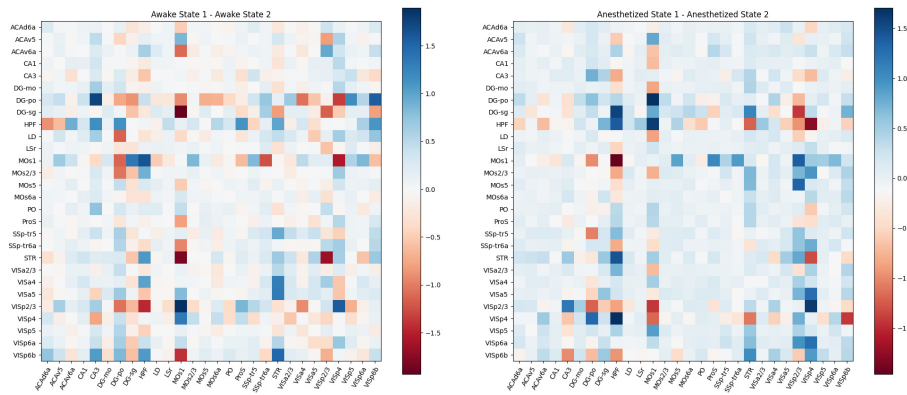


Figure 8.11: Mouse 586468, Difference between Awake states and Anaesthetized states, Current=45uA

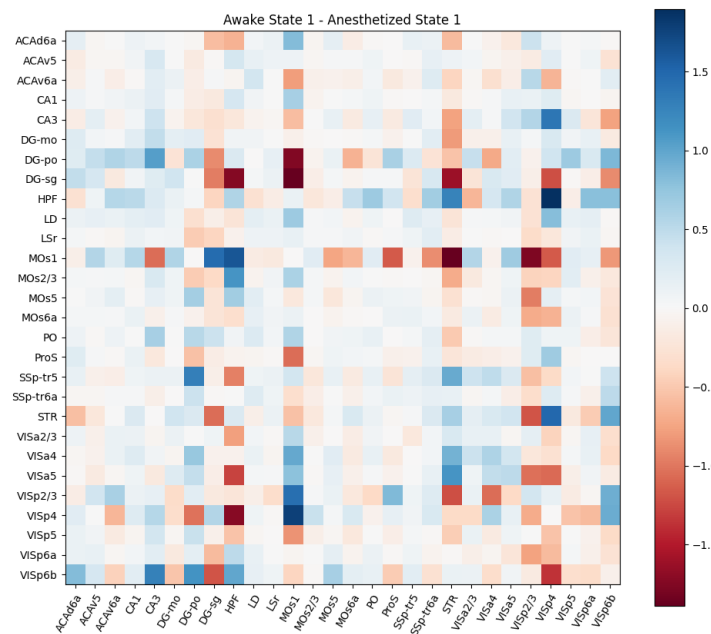


Figure 8.12: Mouse 586468, Difference between Awake and Anaesthetized state, Current=45uA

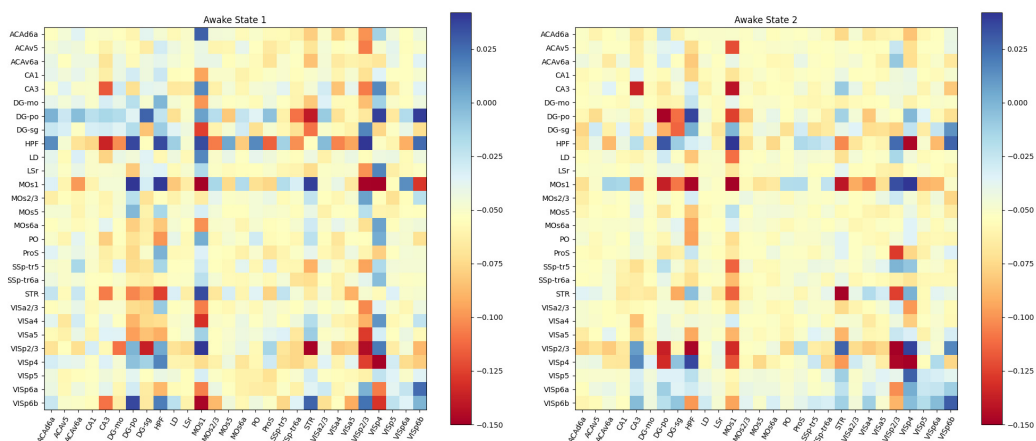


Figure 8.13: Mouse 586468, Awake and Anaesthetized State, Sensory Stimulation

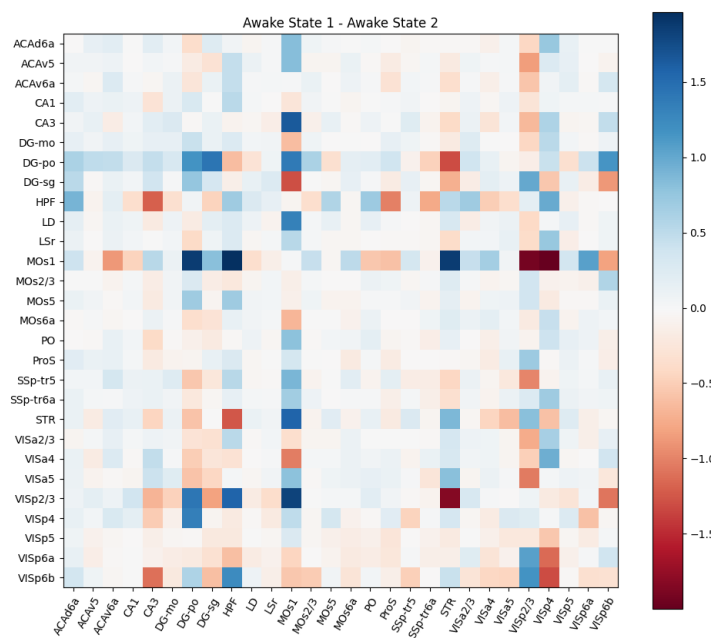


Figure 8.14: Mouse 586468, Difference between Awake states,Sensory Stimulation